Digest Journal of Nanomaterials and Biostructures Vol. 11, No. 4, October-December 2016, p. 1213 - 1229

INVESTIGATIONS ON THE PROPERTIES OF A TWO-DIMENSIONAL NANOPATTERNED METALLIC FILM

C. BREAZU[a,b], N. PREDA[a], M. SOCOL[a], F. STANCULESCU[b], E. MATEI[a], I. STAVARACHE[a], G. IORDACHE[a], M. GIRTAN[c], O. RASOGA[a*], A. STANCULESCU[a]

[a]*National Institute of Materials Physics, 105 bis Atomistilor Street, Bucharest-Magurele, P.O. Box MG-7, 077125, Romania*

[b]*Faculty of Physics, University of Bucharest, Str. Atomistilor nr.405, P.O.Box MG-11, Bucharest-Magurele, 077125 Romania*

[c]*Laboratoire LPHIA, Université d'Angers, LUNAM, 2 Bd. Lavoisier, 49045, Angers, France*

This paper presents some investigations of the effect of nanopatterning on the properties of aluminum layer deposited by sputtering. UV-Nanoimprint Lithography technique has been used for the realization of a 2D array of nanostructures (pillars) in aluminum film characterized by cylindrical shape and the following structural parameters: diameter between 400 nm and 490 nm, depth between 320 nm and 420 nm and periodicity of 1.1 μm, which have been revealed by SEM and AFM measurements. The UV-Vis transmission, reflection and photoluminescence measurements have evidenced the effect of the nanopatterning on the optical properties of the Al layer.

(Received September 6, 2016; Accepted November 10, 2016)

Keywords: Nanopatterning**,** Aluminum nanostructures, UV-Nanoimprint Lithography, Surface plasmons, Optical properties

1. Introduction

The metallic electrode is a very important part of any electronic and optoelectronic device, including organic devices, such as solar cells, light emitting devices and field-effect transistors.

The performances of the photovoltaic and optoelectronic devices depend on many factors such as: the mechanism of charge carriers generation which is limited by the radiation absorption, charge carriers injection and transport which are limited by the energetic barriers inside the heterostructure, recombination processes which are determined by the device structure and extraction of the generated radiation which is limited by the reflectivity of the metallic electrode. For reducing the charge carriers waste, a solution can be offered by thin active layers increasing the flux of charge carriers by increasing the intensity of the electric field and reducing the recombination of the generated charge carriers. But the thin films are not assuring an increase in the absorbed radiation involved in the charge carrier's generation. An alternative to this problem could be offered either by a network of (nano) structures developed in the metal layer or a nano material (nanoparticles) fixed at the interface metal-organic [1,2].

The recent advances in the nanotechnology domain offer the possibility for controlling the properties of the metallic surfaces in structures having dimensions lower than the wavelength using the nano-patterning [3,4].

By 2D nanopatterning of the metallic electrode it is generated a periodically array (network) of (nano)structures and the behavior of the light can be modified by the generation of the plasmonic phenomena [5,6]. The presence of surface plasmon polaritons (SPPs) moving along the electrode surface can generate phenomena controlled by the shape and dimension of the (nano)structures [7]. Phenomena like the resonance of the surface plasmons or resonant interaction between the surface plasmons and the incident photons favor two effects: a significant reduction of

* Corresponding authors: oana.rasoga@infim.ro

the metal reflectivity because the photons are absorbed by the surface plasmons and an enhancement of the local optical field intensity because of the photons energy stored by the surface plasmons.

Both optical effects (improved radiation absorption efficiency by ”light trapping”) and electrical effects (intense electric field determining an increased mobility of the carriers and enhanced area of the metal-organic contact favoring carriers injection/collection) can be generated applying the nanopatterning to the metallic contact in an organic heterostructure.

Aluminum (Al) has been selected as metal because it is abundant, cheaper than the noble metals and the nanostructured Al shows interesting plasmonic effects [8,9].

In the case of structures having dimensions lower than the wavelength of the incident photons, the evanescent electromagnetic field is confined for the radiation frequency situated close to the plasmon resonance frequency. This way the surface plasmonic polarons can efficiently trap and guide the light in the next deposited layer, which is an organic semiconductor in organic devices. This way the nanostructuring allows redirecting the absorbed beam alongside the separation interface assuring an absorption length that is order of magnitude higher than the optical absorption in the layer thickness.

This paper presents a comparative study between the properties of an Al non patterned and patterned with a 2D periodic array of (nano)structures layer deposited by sputtering on different substrates. We have used the UV-Nanoimprint Lithography for the realization of the 2D patterned nanostructures characterized by shape and structural parameters such as diameter and depth. The patterning characteristics are determined by the processing conditions related to spin coating, soft stamp geometry and contact mode parameters. These characteristics of the 2D array of structures have been revealed by SEM and AFM measurements. The effect of the Al layer patterning on the UV-Vis transmission, reflection and photoluminescence spectra has been evidenced.

2. Experimental

Large-area nanopatterning technology is considerate to be important for many applications, such as optoelectronics, nanophotonics, optics because it can increase the performance of devices and products, such as organic solar cells, light emitting diodes (OLEDs), field effect transistors (OFETs), laser diodes, displays etc.

To obtain 2D nanoholes structured metallic layer we have used the UV Nanoimprint Lithography (UV-NIL) technique that is a nonconventional nanopatterning method for producing complex structures from micro-to nanoscale with high precision, at low cost, in a wide variety of materials. In contrast to the conventional technique electron beam lithography (EBL), which has a low throughput for a mass production and use photons or electrons to modify the chemical properties of resist, NIL is focused on the direct mechanical and physical deformation of the resist, assuring significantly high resolution and feasibility for mass fabrication. Therefore NIL is a promising technology that enables the patterning of large area in the wavelength range. This is a low cost, high throughput, high resolution lithography technique already utilized for the surface nanopatterning to assure the light trapping in thin film crystalline silicon solar cells [10,11].

In this technique a transparent mold with predefined surface relief nanostructures on its surface is put in direct contact and used to deform a thin resist film or an active material deposited on a substrate followed by a hardening step to preserve the shape of the structure [4]. UV-NIL is based on the direct contact between mold and resist deposited on different substrates, which can be UV- cured (solidified), by applying an uniformly controlled contact force [12,13]. The flexible mold is the key element responsible for patterning area, resolution, throughput and uniformity of the imprinted pattern [14]. Usually the soft mold is a bi-layer structure made of a rigid glass backplane for ensuring mechanical stability and a patterned soft PDMS (the commercially available PDMS brand Sylgard 184 from Dow Corning Inc.) imprint layer that adapts perfectly to the waviness or bow of the substrate [14]. The NIL process was very simple and included four steps (Fig. 1): a) firstly, UV-resist is spin-coated at room temperature on clean glass or Si substrate covered by a ”primer” or adhesion promoter; b) the mold (soft stamp) that contains the relief nanostructures is brought into direct contact with resist on the substrate with a certain pressure; c)

after the mold and the resist were brought into contact the resist is solidified by exposure to UV light radiation source, d) finally the mold is removed, leaving the UV-curable resist patterned [14].

The UV-NIL process is realized in our experiments with a EVG 620 mask aligner, Brewer Science Cee 200X Spin Coater for the deposition of adhesion promoter and UV-curable resist layer, and an EVG soft stamp designed for obtaining pillars nanostructures in the imprinted resist layer.

The soft stamp provided by EV Group is the negative for nanostructuring with cylindrical pillars with ϕ=400 nm and distance between the centers of two neighboring pillars of 1.1 μm. We have used as substrates glass slices of 90 mm x 90 mm and 4 inches one side polished single crystal Si. The substrates have been ultrasonically cleaned in water with detergent for 5 min, acetone for 5 min and isopropyl alcohol for 5 min before imprinting.

The first step in achieving nanostructures consists in preparing the substrate and deposition of the UV-resist over it. For a better fixation of the resist on substrate, the substrate is thermally treated and subsequently is covered by a layer of adhesion promoter (primer). The glass or Si substrates were heated at 150^0 C for 2 min on a hot plate. After this the adhesion promoter is applied dynamically on substrate by spin-coating. The next step is the deposition of the resist by spin coating on the top of the adhesion promoter. The substrate is thermally treated on a hot plate at 120 ^{o}C for 2 min after the deposition of primer and at 120 ^{o}C for 30 s after the deposition of UV-resist. The soft stamp containing the model for nanostructuring is placed over the resist material using a controlled uniform contact pressure which can be varied between 50 mbar and 950 mbar. The soft stamp and substrate coated with adhesion promoter and resist were brought into contact and after this the resist is solidified by UV-exposure for 90 s. The last step is to remove the stamp from the substrate, leaving on substrate the desired pattern.

Using this process we have obtained 6 samples of patterned Al layer on Si successively covered by a film of primer and a film of UV-resist (PR) in 6 different sets of experimental conditions (Table 1) and 1 samples of patterned Al layer on glass successively covered by films of primer and PR.

Table 1: Experimental conditions for PR patterning by UV Nanoimprint Lithography.

Sample	Adhesion promoter layer				UV-resist layer				Vacuum contact pressure (mbar)
	Stage 1		Stage 2		Stage 1		Stage 2		
	Speed (rpm)	Time (s)	Speed (rpm)	Time (s)	Speed (rpm)	Time (s)	Speed (rpm)	Time (s)	
SiP1	1000	20	2000	30	1000	5	2000	30	50
SiP2	1000	1	2000	30	1000	1	3000	30	50
SiP3	1000	1	2000	30	1000	1	3000	40	100
SiP4	1000	1	2000	30	1000	1	3000	40	100
SiP5	1000	1	2000	30	1000	1	2000	40	200
SiP6	1000	1	2000	30	1000	1	3000	40	300
glassP1	1000	1	2000	30	1000	1	3000	30	100

We have obtained a 2D periodic array of pillar/holes nanostructures in resist layer, characterized by a periodicity of 1.1 μm measured between the centre of two successive pillars and cylindrical shape with diameter between 250 and 410 nm and depth between 250 and 350 nm, determined by the processing conditions related to spin coating, soft stamp and contact mode parameters (Table 1).

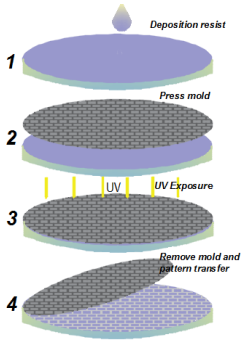

Fig. 1. Process flow of UV-NIL

This technique of nanopatterning has been used to prepared nanostructured Al layer able to produce plasmonic resonance in visible [15]. Al film has been deposited on the all surface of nanopatterned resist by sputtering utilizing a UHV-Deposition System (Bestec) and the following deposition parameters: pressure in the chamber=1x10^{-7} mbar, duration of deposition=2 hours. The thickness of the metallic film was ~ 70-80 nm.

The optical properties of the nanopatterned samples have been investigated by comparison with those of the non patterned samples. For drawing the transmission spectra we have used a Carry 5000 Spectrophotometer in the spectral range 200-1500 nm and for the reflection spectra a Perkin-Elmer Lambda 45 UV-VIS spectrophotometer equipped with an integrating sphere with illumination at 8^{o} in the spectral range 250-950 nm. The photoluminescence spectra have been drawn with an Edinburg Instruments F-900 Spectrofluorometer in the following conditions: $\lambda_{excitation}$=335 nm, measurement range=350-650 nm, slit=2, step=1; $\lambda_{excitation}$=435 nm; measurement range= 450-850 nm, slit=2, step=1.

The surface and cross-section morphology of the patterned layers (PR, Al) deposited on Si and glass was investigated by SEM using a Zeiss EVO 50XVP microscope at an acceleration voltage V_{acc}=20 kV and different magnification 15.00kX, 40.00kX, 50.00kX, 100.00kX. From the SEM images can be evaluated the depth/height and width of the holes/pillars, and the periodicity of the 2D array of structures.

Details about the surface topography of the 2D array of holes/pillars obtained in the PR layer have been evidenced by AFM with a MultiView 4000 Nanonics working in tapping mode and phase feedback, with a tuning fork probe having the following characteristics: $\phi_{aperture}$=20 nm, $\nu_{resonance}$=38 kHz and active quality factor Q=1800. From the profile line we have evaluated the geometrical details related to depth/height and width of the holes/pillars for the 2D periodic array.

3. Results and discussion

SEM images have revealed the geometrical particularities of the 2D array of structures developed in the patterned PR and Al layer deposited on patterned PR. The morphology of patterned PR is characterized by the presence of cylindrical pillars with diameter between 250 nm and 410 nm and periodicity ~1.1 μm (Table 2). When a layer of Al is deposited on the periodic network patterned in UV-resist deposited on Si the developed pillars have a diameter between 400 nm and 490 nm and periodicity of ~1.1 μm (Table 2).

Table 2: Geometrical parameters of 2D array of pillars/holes developed in PR and Al layers.

Sample	Pillar diameter (nm)	Periodicity (μm)	Hole diameter (nm)
SiP1	395	1.099	703
SiP1/Al	480	1.097	625
SiP2	249	1.101	852
SiP2/Al	340	1.100	765
SiP3	405	1.101	696
SiP3/Al	490	1.101	610
SiP4	333	1.085	752
SiP4/Al	455	1.096	641
SiP5	410	1.107	697
SiP5/Al	404	1.091	687
SiP6	352	1.093	742
SiP6/Al	434	1.090	656
glassP1/Al	395	1.087	692

Typical SEM images (including cross section images) have revealed the characteristics of the PR layer deposited on Si patterned with pillars/holes (Fig.2 and Fig.3), Al layer deposited on patterned PR (Fig.4) and Al layer deposited on patterned PR deposited on glass (Fig.5). We have evidenced the development in the PR deposited on Si of an uniform 2D periodic network (Fig.2a-c) and regular frustoconic shape of the holes/pillars (Fig.2d,e).

To measure the depth/height of the hole/pillar the Si substrate was cut along a row of pillars and examined with a scanning electron microscope. The structure looks like an array of rectangular pillars with the top of the pillars rounded.

The nanostructures of 2D periodic array are characterized by depth between 250 nm and 350 nm (Fig.2e) and (Fig.5d).

We have also evidenced that the density of defects revealed on the patterned PR surface decreased with increasing the vacuum contact pressure from 100 mbar sample SiP4 (Fig.3,a) compared to 300 mbar sample SiP6 (Fig.3,c). A regular 2D network has been obtained in sample SiP3 (Fig.2,c-e) realized at 100 mbar compared to samples realized at 50 mbar. This means that a higher pressure favoured the generation of a better patterning of the surface for the samples SiP6 and SiP3.

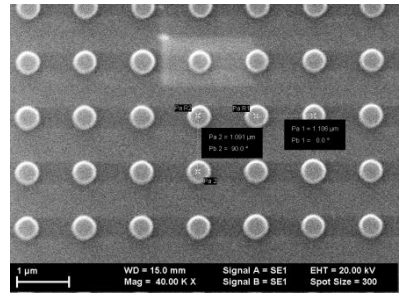

SiP1(a)

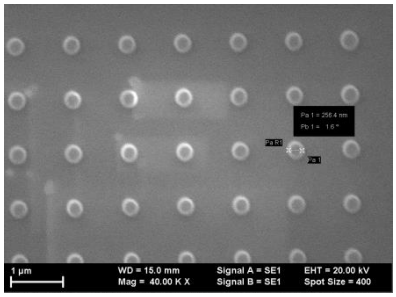

SiP2(b)

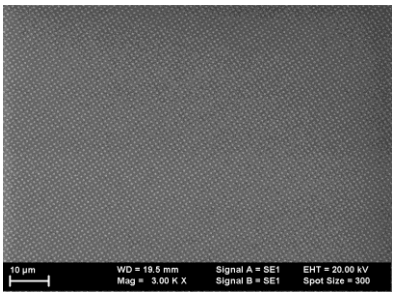

SiP3 (c)

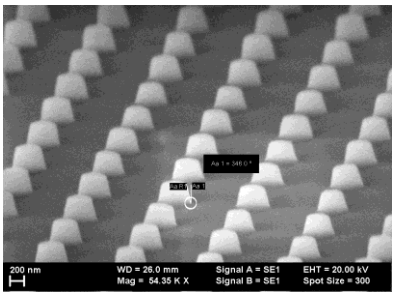

SiP3 (d)

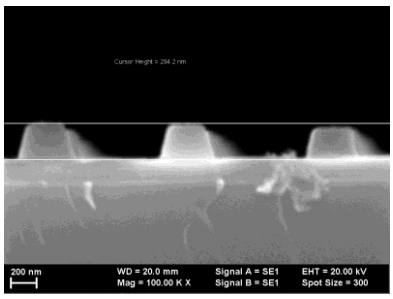

SiP3 (e)

Fig. 2 SEM images (a-c) and cross section SEM images (d,e) of patterned PR deposited on Si.

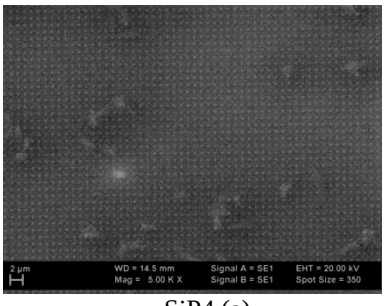

SiP4 (a)

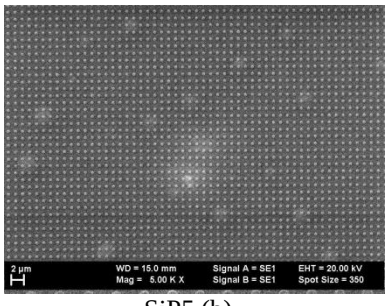

SiP5 (b)

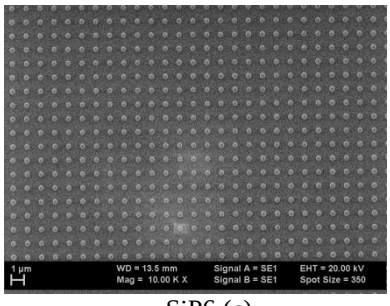

SiP6 (c)

Fig. 3 Large area SEM images of PR deposited on Si and patterned at different vacuum contact pressure: 100 mbar/SiP4 (a), 200 mbar/SiP5 (b), 300 mbar/SiP6 (c).

When the adhesion promoter and PR layers are deposited in the same experimental conditions (SiP4 and SiP6), the increase by 3 times of the contact pressure has determined a small decreasing effect on the diameter of the holes, from 752 nm to 742 (Fig.4a,c) and Table 2. The smaller diameter of the hole has been obtained in the structures patterned in the thicker PR (determined by a lower rotation speed in stage 2 of spin coating, Table 1), SiP5 (Fig. 4b) and Table 2.

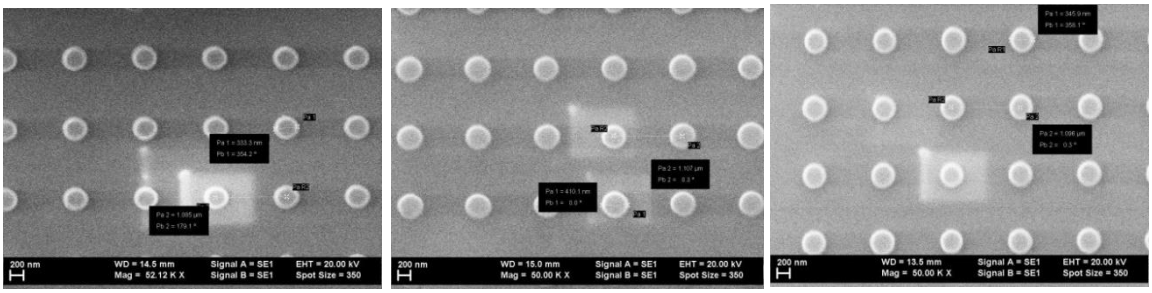

SiP4 (a) SiP5 (b) SiP6 (c)

Fig. 4: Typical SEM images of PR layer deposited on Si and patterned at different vacuum contact pressure: 100 mbar/SiP4 (a), 200 mbar/SiP5 (b), 300 mbar/SiP6 (c).

By the deposition of Al layer (~ 70-80 nm) the shape of the pillars/holes became irregular with inflorescence (boules) shape. The shape is determined by the clusters generated during the deposition of Al on organic film. The diameter of the pillar is between 405 nm and 490 nm and the height between 320 nm and 420 nm, at a periodicity of ~ 1 μm (Fig.5).

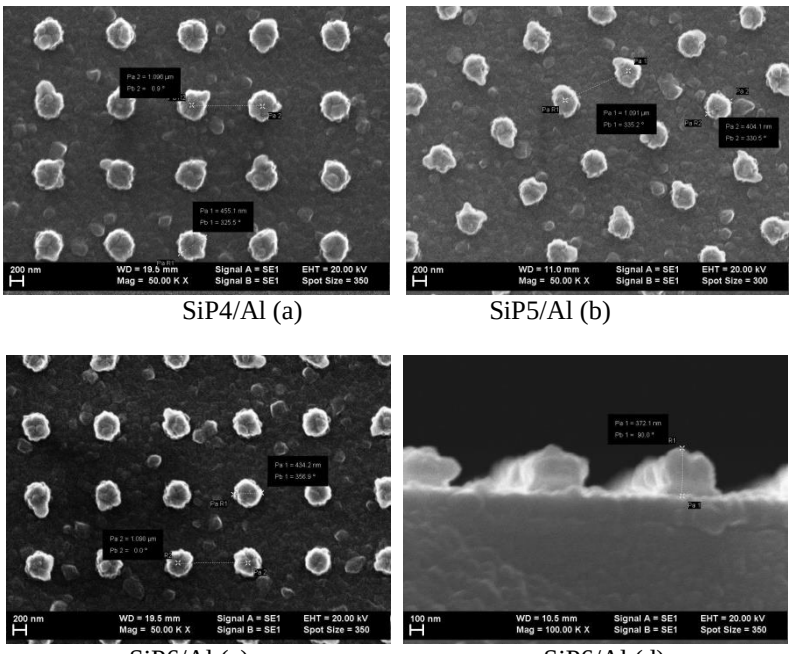

SiP4/Al (a) SiP5/Al (b)

SiP6/Al (c) SiP6/Al (d)

Fig. 5. Typical SEM images of patterned PR deposited on Si and covered by Al layer.

The deposition of Al on the patterned PR is a relatively hard process which can affect the patterning of the polymeric layer and can even determine the exfoliation of the layer (Fig.6a). If the Al layer is deposited on patterned PR covering the Si substrate at high vacuum contact pressure (300 mbar) we can evidence large area of the patterned metallic layer with no deterioration/degradation of the patterning (Fig.6b).

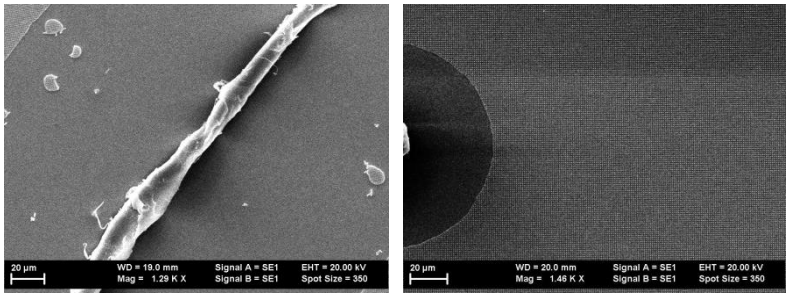

SiP4/Al (a) SiP6/Al (b)

Fig. 6: SEM images of Al patterned layer revealing the presence of large defects areas.

The periodic structure developed in Al film deposited on patterned PR spin coated on glass shows a pillar's diameter of 395 nm and a periodicity of 1.1 µm, evidenced on SEM images (Fig.7). We have used the same soft stamp for the preparation of all the patterned samples. A specific surface morphology characterized by the presence of boules of different dimension has been evidenced for Al deposited on patterned PR on glass substrate (Fig.7) as for Al deposited on patterned PR on Si substrate.

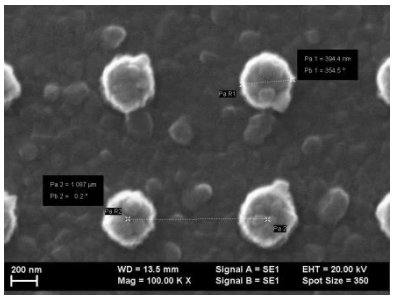

Fig. 7. SEM images of Al layer deposited on nanopatterned PR covering glass substrate.

A typically AFM image of nanopatterned PR deposited on Si substrate (SiP2 sample) shows a large area uniform patterning of the surface with rows of isolated, well defined holes/pillars (Fig.8).

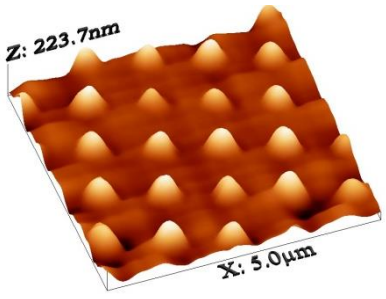

Fig. 8. AFM 3D image of a nanostructured PR layer deposited on Si substrate (SiP2).

We have evaluated the distance between the pillars (periodicity) of the 2D array and the depth of the hole from the profile line drawn in different direction on the patterned surface.

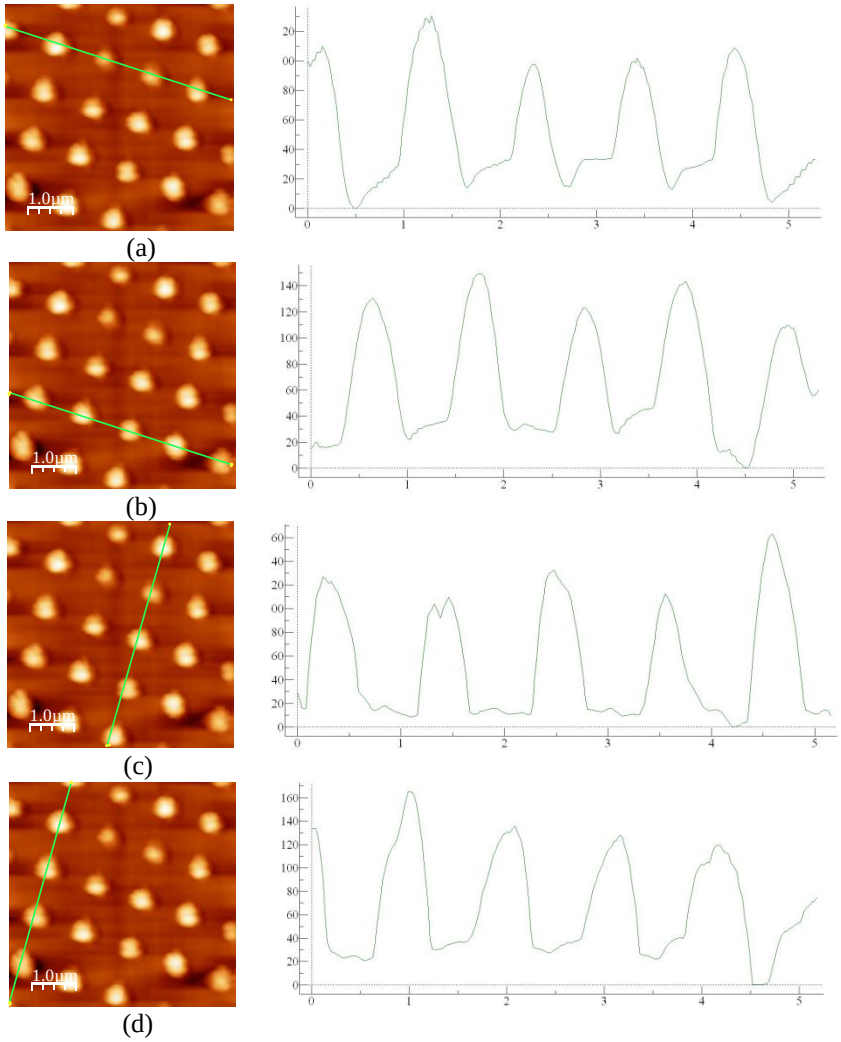

Fig. 9. Profile lines on sample SiP2 where OX represents position in µm and OY represents height in nm.

We have remarked on these images an asymmetry in the shape of the holes and differences in the diameter of the holes situated on a given direction, which can be related to the periodicity of the 2D array and in the depth of the nanostructures, which can be related to the position of the bottom of the holes. The average values of the periodicity evaluated from the position of the middle of two successive peaks is ~1.1 µm in concordance with the values obtained by SEM measurements. The average diameter evaluated at the top of the pillars for a given direction from AFM measurements is between 225 nm and 280 nm for the four selected directions (Fig. 9), with an average value of ~ 250 nm for the entire scanned area in concordance with SEM measurements (Table 2, sample SiP2). The information about the depth of the holes obtained from AFM is not relevant because it is possible that the tip of the probe does not touch the bottom of the hole during the measurement. Therefore, for comparison with SEM measurements, we consider the diameter at the top of the pillars.

The transmission spectrum shows an average transmission of the glass substrate of 89 % in the range 350 nm - 900 nm and a slightly lower transmission of PR (Fig.10).

We have investigated the optical properties of the two-dimensional periodic nanopatterns developed in the PR layer using as reference a non-patterned PR film. The transmission spectrum of the 2D array developed in the polymeric PR deposited on glass covered by primer shows a shape suggesting the presence of a stronger scattering phenomenon between 350 nm and 750 nm compared to the reference glass or glass covered by PR layer (Fig.10).

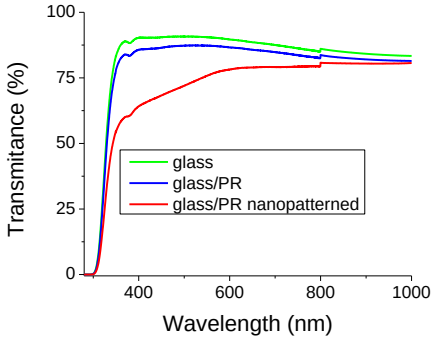

Fig. 10. Comparative UV-Vis transmission spectra of non-patterned and patterned PR.

We have also investigated the transmission properties of the Al layer deposited on the 2D array of structures obtained by the nanopatterning of PR compared with the reference non patterned Al layer (Fig.11).

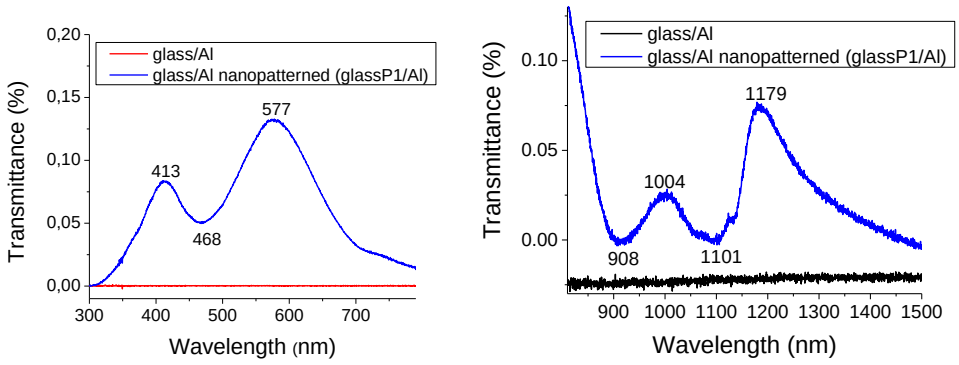

Fig. 11. Comparative UV-Vis transmission spectra of non-patterned and patterned Al layer.

A very low transmission in the domain 300-800 nm has been evidenced on the layer of Al deposited by sputtering on non-patterned PR. This behavior can be explained by the large value of the imaginary part of the dielectric function in the visible range and high plasmon frequency in UV region of Al [16], the most of the incident light being reflected by the Al film. We have evidenced a significant enhancement in transmission in our samples with the Al layer perforated, showing a 2D array of Al nanostructures which can be considered as apertures for incident light (Fig.11). When light falls onto a thin metal film are excited the surface plasmons which accumulate much energy around the holes (apertures) and in consequence the electric field penetrates the metal. The surface plasmons on the other side of the metal film convert the energy into light. Therefore the surface plasmons direct the light towards the holes and it is assured the transmission of more light than it is expected [17-19].

Because the diameter of hole is large, around 700 nm, much larger than the distance between the edges of two neighbor holes, ~ 400 nm, the absorption (loss) in the aluminum volumes is not so strong and the transmission of light becomes significant. The transmission through our irregularly shape holes is sustained by the surface plasmons excited by light incident on the holes array and their lateral propagation [17]. A possible mechanism to explain the nature of the surface plasmons interaction with the holes, already proposed in earlier investigations of far-infrared transmission through hole arrays [18], is the coupling of the plasmons on the two surfaces of the metallic film through the 2 D array of holes [19] because the film thickness in the holes' areas is smaller than the penetration depth of the surface plasmons [19].

An enhancement of the optical transmission has been evidence in our Al optically thick (thickness ~ 70-80 nm) nanopatterned films deposited on glass with peaks situated at the

resonance wavelength, namely when the frequency of the incident electromagnetic field matched the frequency of the plasmons generated in the nanostructured metallic layer. Such metallic structures reject the visible spectrum except for selective transmission bands which are associated with the excitation of surface plasmon polaritons (SPPs) [20]. The position of these transmission bands is determined by the geometrical parameters such as the array periodicity, shape and size of the nanostructures. The position of the enhanced transmission peaks can also be modified by changing the diameter of the hole [16]. In our 2D arrays prepared by UV-NIL we have obtained transmittance bands with peak situated in Vis at 413 nm and 577 nm (Fig.11). Al satisfy the condition for collective oscillations of the free electrons gas in nanostructures namely localized surface plasmon resonance (LSPR) because it is characterized by large negative dielectric real parts over a wide visible wavelength region and small dielectric imaginary part (dielectric permittivity<0) [8].

The holes arranged in a two-dimensional network within an Al layer show a strong increase in transmittance of 2-3 orders of magnitude in nanopatterned layer both at 413 nm (from $5x10^{-4}$ to $8x10^{-2}$) and 577 nm (from $2x10^{-4}$ to $1.3x10^{-1}$).

By structuring aluminum surfaces it is also possible to change the absorbance over a broad range of wavelengths situated in visible domain. An increase in absorbance is evidenced in the region where the transmission decreases: 470 nm, 904 nm and 1100 nm (Fig. 11 and Fig. 12). A decrease has been evidenced in the absorbance of the incident radiation illuminating a 2D array structured Al layer compared to unstructured Al layer (Fig. 12) at the wavelengths where the transmission increases.

The Al layer has a strong intrinsic absorption at 832 nm determining a suppression of the absorbance in the 2D array of structures around this wavelength (Fig.11).

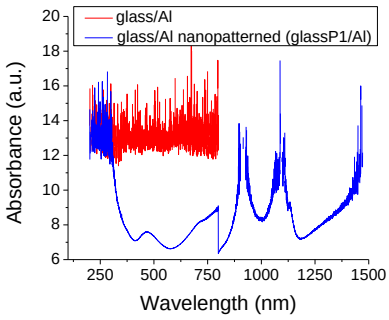

Fig. 12. Absorbance spectra of glass substrate covered by Al and Al nanopatterned layer.

We have drawn the plot R as a function of λ, where R is the absolute reflectance. Analyzing the reflectance and transmittance spectra of Al layer on glass we have remarked that in the region where the intensity of the light reflected by the deposited layer reduces, the transmittance of the layer increases (Fig. 11 and Fig.13).

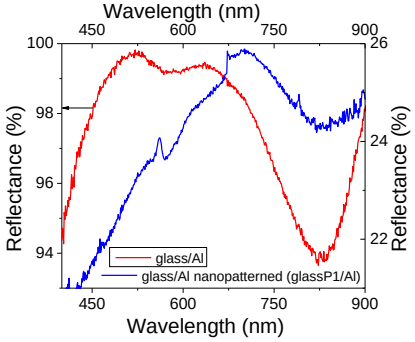

Fig. 13. Reflectance spectra of glass substrate covered by Al layer and Al nanostructured layer.

We have evidence a high decrease in reflectance in the nanopatterned Al layer in the visible range around 21-26 % compared to non patterned Al layer, 94-99 % (Fig. 13), which is determined by the absorption of photons by the surface plasmons through a resonant interaction.

The film of Al shows a strong reflectance of the incident light (Fig.13) which decreases significantly around 830 nm where the intrinsic absorption of Al is very strong. The 2D Al array shows a lower and broader reflectance than the Al non-patterned layer because not only the absorption of light in the metal determines the optical response of the 2D array but also the effects of interference between light reflected from within the holes and the light reflected from the top of the film, and scattering of light inside the holes [21]. The peak in reflection is obtained when the frequency of the incident electromagnetic field matched the frequency of the plasmons generated in the nanostructured metallic layer causing resonance phenomena. Because the area of the flat Al regions between holes is small compared to the volume occupied by the holes, the coupling of the radiation to excitation of plasmons on the surface of the prepared structured film decreases reducing the resonance phenomena. A grating like effect [21] associated with a decrease in reflectivity around the wavelength corresponding to the array's periodicity has not been evidenced.

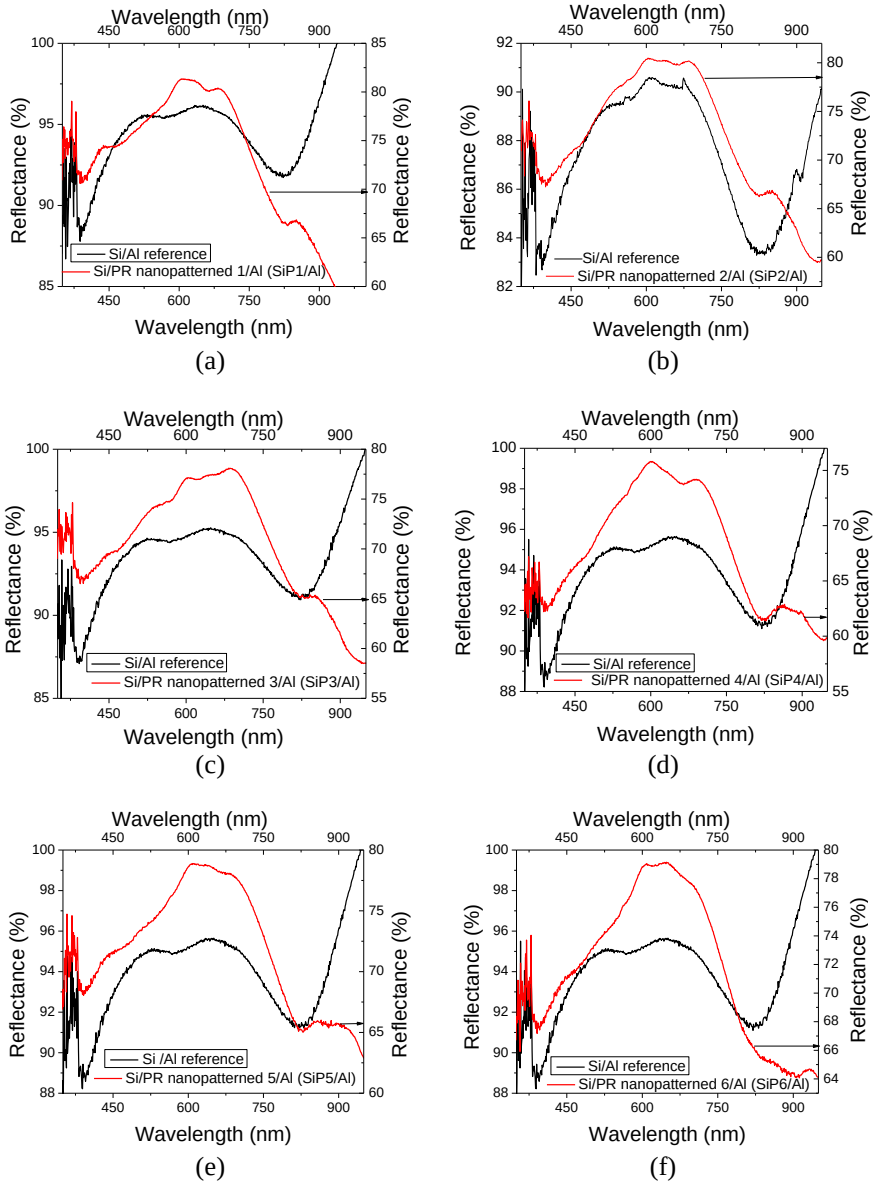

Fig. 14. Reflectance spectra of nanopatterned Al layer compared to non patterned Al layer deposited on Si obtained in different experimental conditions (Table 1).

The behavior of the nanopatterned Al layer deposited on Si (Fig.14) is not very different of that of the nanopatterned Al layer deposited on glass. In the case of nanopatterned Al film, the shape of the reflectance spectra is not determined by interference phenomena taking place in the thin Al film (peaks situated at 520 nm and 670 nm on the spectrum of non patterned Al film deposited on Si) but by resonance phenomena between the frequencies of the surface plasmon generated in Al film and the frequency of the incident radiation. The behavior of the nanopatterned Al layer changes and the shape of the reflection spectra is a consequence of interference and scattering effects determined by the perfection of the 2D array of nanostructures and regularity of the geometrical parameters related to the depth and width of the nanostructures affecting the refractive index. The decrease in reflectance of the nanopatterned film of Al deposited on Si is lower, from 90-95 % to 75-80 %, than the decrease in reflectance of the nanopatterned film of Al deposited on glass, confirming a better quality of the nanopatterning on Si.

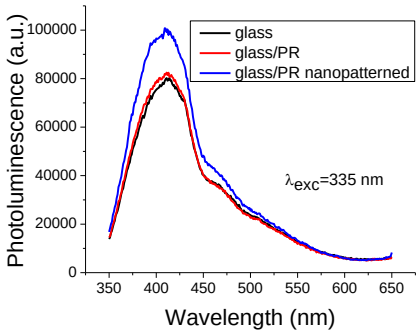

Fig. 15: Emission spectra of glass covered by PR and nanopatterned PR at UV excitation.

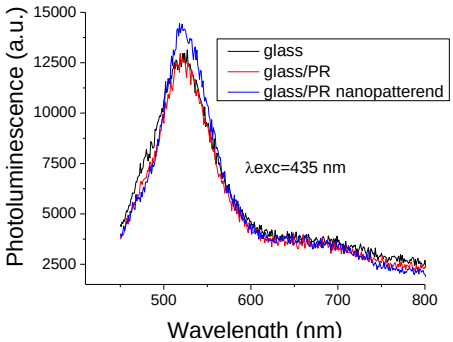

Fig. 16: Emission spectra of glass covered by PR and nanopatterned PR at Vis excitation.

The photoluminescence spectra of PR deposited on glass shows at excitation with λ=335 nm a maximum situated at ~ 410 nm and two weak shoulders at 470 nm and 510 nm (Fig. 15) and at excitation with λ=435 nm a maximum situated at ~ 520 nm (Fig. 16). These peaks could be associated with the intrinsic properties of glass, including the presence of defects. The nanopatterning has increased the PL emission, but has not modified the position of the peak. The PL behavior is determined by the PL properties of the glass.

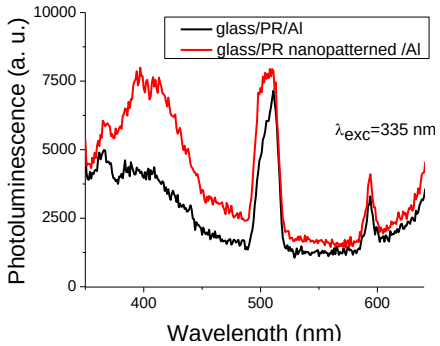

Fig. 17. Emission spectra of nanopatterned Al film compared to Al non patterned film deposited on glass at UV excitation.

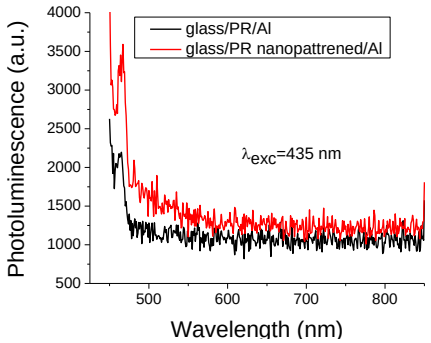

Fig. 18. Emission spectra of nanopatterned Al film compared to Al non patterned film deposited on glass at Vis excitation.

The shape of the emission spectra has changed by the deposition of the Al layer. The band centred at 410 nm for excitation with λ=335 nm preserves and two sharp emission peaks appear at ~510 nm and ~595 nm (Fig.17). These peaks can be associated with resonance phenomena between the energy of incident light and the surface plasmons generated in the metallic layer deposited on PR. An emission peak situated at ~ 470 nm has been evidence in Al layer at excitation with λ=435 nm (Fig.18). The shape is similar in both patterned and non patterned Al layer, being determined by the emission properties of Al layer enhanced by the surface plasmons (Fig. 17 and Fig.18). A slight increase in PL emission has been evidenced after nanopatterning, and this could be attributed to the energy transfer between the nanostructures and surface plasmons [22]. The surface plasmons increase the density of states and the spontaneous emission rate in polymer (PR) leading to an enhancement of light emission (Fig.17 and Fig.18) by surface plasmons-holes coupling [22].

At illumination with λ=335 nm, the emission spectrum of the patterned PR deposited on Si (Fig.19) is different from the emission spectrum of the same layer deposited on glass (Fig.15) and shows a width band centered at ~400 nm and two sharp peaks situated at ~500 nm and 600 nm. At illumination with λ=435 nm the width band situated between 450 nm and 600 nm is preserved (Fig.16 and Fig.20), but in the nanopatterned layer on Si spectrum is superimposed a narrower peak situated around 460-470 nm (Fig.20). This effect is stronger in the thicker layer of PR (determined by the spin coating parameters, Table 1) because of the increased number of emitting entities. The excited PR emits radiation which is amplified by multiple reflections on the walls inside the holes cavities.

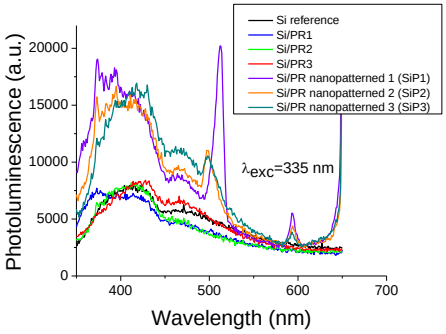

Fig. 19: Emission spectra of nanopatterned PR compared to non patterned PR deposited on Si at UV excitation.

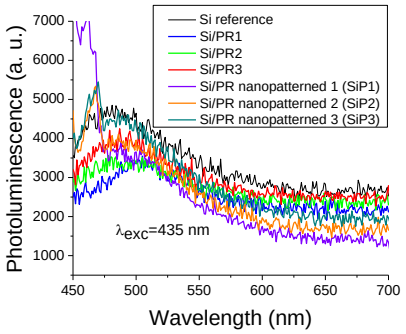

Fig. 20: Emission spectra of nanopatterned PR compared to non patterned PR deposited on Si at Vis excitation.

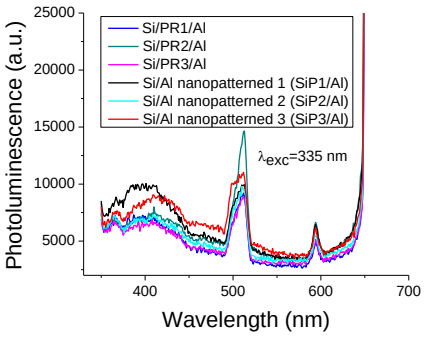

(a)

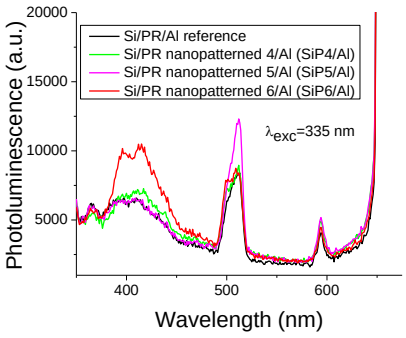

(b)

Fig. 21. Emission spectra of nanopatterned Al film compared to Al non patterned film deposited on Si at UV excitation.

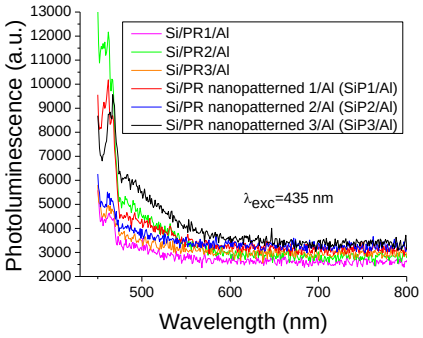

(a)

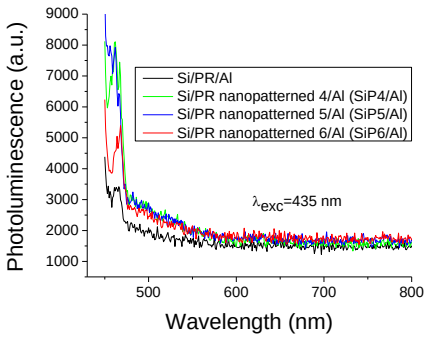

(b)

Fig. 22. Emission spectra of nanopatterned Al film compared to Al non patterned film deposited on Si at Vis excitation.

The nanopatterning of the PR leads to spectral changes through the appearance of maxims which preserve in Al nanostructured layer. The emission of the patterned Al film deposited on Si shows, at illumination with λ=335 nm, a width band centered at ~410 nm and two sharp peaks situated at ~500 nm and 600 nm (Fig.21). At illumination with λ=435 nm, the shape of the PL spectra obtained with nanostructured Al on Si are similar with the spectra of non-structured Al on Si (Fig.22) and is similar with the spectra of nanostructured PR deposited on Si (Fig.20). The peaks situated at 500 nm and 600 nm observed in Al coated samples can not be correlated to Si defects emission, because they are situated in the band gap and correspond to UV emission. Therefore, the emission properties of Al structures developed on Si are determined by the properties of PR on which is deposited the Al film.

The photoluminescence response at illumination with λ=335 nm or λ=435 nm of Al 2D array of structures is independent on the substrate used for deposition glass or Si. The PR nanostructuring conditions can affect the properties of the 2D array of nanostructures developed in Al layer.

4. Conclusions

UV-Nanoimprint Lithography has been used to obtained a 2D periodic array of pillars/holes nanostructures in an UV-resist layer deposited on different substrates (glass, Si), characterized by a periodicity of 1.1 μm. These nanostructures have a cylindrical shape with diameter between 250 nm and 410 nm and depth between 250 and 350 nm in correlation with the processing conditions related to spin coating, soft stamp and contact mode parameters. Al film with thickness around 80 nm has been deposited by sputtering on the surface of patterned UV-resist and the optical properties of the patterned Al film have been investigated by comparison with those of the non patterned Al film. After the deposition of Al on the periodic network patterned in UV-resist deposited on Si the developed pillars have a diameter between 400 nm and 490 nm and periodicity of 1.1 μm with irregular shape determined by the characteristics of the Al deposition on organic generating clusters. SEM images have revealed the development of a uniform 2D periodic network of regular frustoconic shape pillars/holes. We have also evidenced that a higher vacuum contact pressure favored the generation of a better patterning of the surface, characterized by a lower density of defects. The vacuum contact pressure is a critical parameter because it affects not only the geometrical characteristics of the patterning but also the quality of patterning. A significant increase in the contact pressure and thickness of the UV-resist has slightly decreased the diameter of the holes. The diameter and periodicity of the holes developed in UV-resist deposited on Si, obtained by SEM are confirmed by AFM measurements. The SEM images of the structures developed in Al deposited on glass substrate have revealed a pillar's diameter of 395 nm and a periodicity of 1.1 μm.

An enhancement of the optical transmission has been evidence in our Al optically thick nanopatterned films deposited on glass with peaks situated at the resonance wavelength, 413 nm and 577 nm, which are associated with the excitation of surface plasmon polaritons. The increase in transmission in nanopatterned Al layer is associated with a decrease in absorbance/reflectance.

The behavior of the nanopatterned Al layer changes, the and the shape of the reflection spectra is a consequence of interference and scattering effects determined by the perfection of the 2D array of nanostructures and regularity of the geometrical parameters. The decrease in reflectance of the nanopatterned film of Al deposited on Si is lower than the decrease in reflectance of the nanopatterned film of Al deposited on glass, confirming a better quality of the nanopatterning on Si.

We have evidenced a decrease in reflectance in nanopatterned Al film. The coupling of the radiation to excitation of plasmons on the surface of the Al structured film decreases reducing the resonance phenomena, because the flat Al regions between holes is small compared to the volume occupied by the holes.

The photoluminescence response of Al 2D array of structures is independent on the substrate used for realization of nanostructures, glass or Si, both at illumination with λ=335 nm or λ=435 nm. The PR nanostructuring conditions can affect the properties of the 2D array of nanostructures developed in Al layer.

Acknowledgments

This research was financially supported by Bilateral Collaboration Romania-France project no. 783/2014, Romanian Ministry of Education and Research through Core Founding Program, Contract PN16-480102 and PN-II-PT-PCCA-2011 project no. 153/2012.

References

[1] X. Chen, X. Yang, W. Fu, M. Xu, H. Chen, Materials Science and Engineering **B 178**, 53 (2013).

[2] C. Ma, W. Qin, X. Xu, M. Li, X. Han, L. Yang, S. Yin, J. Wei , F. Zhang , Solar Energy Materials & Solar Cells **109**, 227 (2013).

[3] E. Gondek, P. Karasin , Optics & Laser Technology **48**, 438 (2013).

[4] B. Zeng, Q. Gan, Z. H. Kafafi, F. J. Bartoli, J. Appl. Phys. **113**, 063109 (2013).

[5] C. Shemelya, D. F. DeMeo, and T. E. Vandervelde, Applied Physics Letters **104**, 021115 (2014).

[6] P. Spinelli, V. E. Ferry, J. van de Groep, M. van Lare, M. A. Verschuuren, R. E. I. Schropp, H A Atwater and A Polman, J. Opt. **14,** 024 (2002).

[7] K. Zhou, Z. Guo, S. Liu, J.-H. Lee, Materials **8**, 4565 (2015).

[8] A. S. Mahmood, K. Venkatakrishnan, B. Tan, Nano. Res. Lett. **8**, 477 (2013).

[9] C. Genet, T. W. Ebbesen, Nature **445**, 39 (2007)

[10] I. Abdo, C. Trompoukis, J. Deckers, V. Depauw, L. Tous, D. Van Gestel, R. Guindi, I. Gordon, O. El Daif, EEE J. Photovoltaics, **4**(5), 1261 (2015).

[11] E.-C. Wang, S. Mokkapati, T. P. White, T. Soderstrom, S. Varlamov, K. R. Catchpole, Prog. Photovolt. Res. Appl. **22,** 587 doi:10.1002/pip.2294 (2014).

[12] L. Jay Guo, Adv. Mater. **19**, 495 (2007).

[13] EVG Micro and Nanostructure Manufacturing Guidelines using Imprint Techniques, http://www.microfluidicsinfo.com/EVGguidelines.pdf.

[14] H. Lan, Soft UV Nanoimprint Lithography and Its Applications, Chapter 7

[15] B. Choi, M. Iwanaga, H. T. Miyazaki, K. Sakoda, Y. Sugimotoa, J. Micro/Nanolith. MEMS MOEMS **13**(2), 023007 (2014).

[16] J. F. Zhu, B. Q. Zeng, Z. Wu, J. of electromagn. Waves and Appl. **26**, 342 (2012).

[17] A. Nesci, O. J. F. Martin, „Optical nano-imaging of metallic nanostructures", Proc. SPIE 59280U-1, „Plasmonic nanoimaging and nanofabrication" Eds. S. Kawata, V. M. Shalaev, D. P. Tsai, doi: 10.1117/12.616932

[18] D. E. Grupp, H. J. Lezec, T. Thio, T. W. Ebbesen, Adv. Mater. **11**, 860 (1999).

[19] F. Keilmann, Int. J. of Infrared and Millimeter Waves **2**, 259 (1981).

[20] M. Ye, X. L. Hu, L. B. Sun, B. Shi, Y. Xu, L. S. Wang, J. Zhao, Y. Q. Wu, S. M. Yang, R. Z. Tai, J. Z. Jiang, D. X. Zhang, J. Alloy and Compounds **621**, 244 (2015).

[21] P. N. Bartlett, J. J. Baumberg, S. Coyle, M. Abdelsalem, Faraday Discuss. **125**(19), 16 (2003).

[22] K. Okamoto, I. Niki, A. Shvartser, Y. Narukawa, T. Mukai, A. Scherer, Nature Materials **3**, 601 (2004).